Gambogenic acid induces cell growth inhibition, cell cycle arrest and metastasis inhibition in choroidal melanoma in a dose-dependent manner

FENGHUA LI, YANSA WANG and YING YAN

Department of Ophthalmology, Linyi People's Hospital, Linyi, Shandong 276000, P.R. China

Received December 1, 2015; Accepted December 1, 2016

DOI: 10.3892/etm.2017.4252

Abstract. The aim of the present study was to explore the effects of gambogenic acid (GNA) on the malignant behaviors of choroidal melanoma cells, including cell viability, cell cycle, migration and invasion, and to elucidate the underlying regulatory mechanism. The human choroidal melanoma cell line OCM-1 was treated with different concentrations of GNA and cell viability, colony formation ability, cell cycle, migration and invasion were analyzed. Additionally, cells were incubated with or without LY294002, a specific inhibitor of the phosphoinositide 3-kinase (PI3K)/protein kinase B (Akt) signaling pathway, for 24 h. Levels of cell cycle-associated proteins (cyclin D1, cyclin E, cyclin-dependent kinase 2 and P21), epithelial-mesenchymal transition (EMT)-associated molecules (epithelial-cadherin, α-smooth muscle actin and vimentin) and phosphorylated (p)-AKT/AKT were determined using reverse transcription-quantitative polymerase chain reaction and western blot analysis. The results demonstrated that GNA significantly inhibited cell viability and induced cell cycle arrest at the G0/G1 phase in a dose-dependent manner ($P<0.01$). Furthermore, GNA administration significantly suppressed cell migration and invasion in a dose-dependent manner ($P<0.01$). Treatment with GNA or LY294002 induced a marked decrease in the expression of p-AKT/AKT, a significant downregulation in cell cycle-associated molecules ($P<0.01$), and a significant decrease in cell viability ($P<0.01$). Co-treatment with LY294002 and GNA had an additive effect on the growth of OCM-1 cells. In conclusion, the results of the present study suggest that treatment with GNA may inhibit cell viability and induce G0/G1 arrest. Furthermore, GNA may also inhibit cell metastasis via regulating EMT-associated molecules. The PI3K/Akt signaling pathway may be a key mechanism involved in the progression of choroidal melanoma, and GNA may serve as a potential therapeutic reagent for the treatment of this disease.

Correspondence to: Dr Ying Yan, Department of Ophthalmology, Linyi People's Hospital, 27 Jiefang Road, Linyi, Shandong 276000, P.R. China
E-mail: yanying7327@126.com

Key words: gambogenic acid, choroidal melanoma, growth, cell cycle arrest, metastasis

Introduction

Choroidal melanoma is a serious primary intraocular malignant tumor that occurs in adults (1). The incidence of malignant melanoma has been demonstrated to be increasing worldwide (2). Choroidal melanoma is fatal in ~50% of patients due to its latency and metastatic potential, and the principal target organ for metastasis is the liver (3,4). Early detection and therapy is important for improving the prognosis of patients (5); however, the underlying molecular mechanisms of disease development remain to be elucidated.

Gambogenic acid (GNA; $C_{38}H_{46}O_9$; molecular weight, 646.32 kDa) has recently been recognized as a type of antitumor drug (6). GNA is a polyprenylated xanthone, which is isolated from the gum resin gamboge and has a structure similar to gambogic acid (GA) (7). It has been reported to have an inhibitory effect on many types of cancer cells via inhibition of proliferation, metastasis, and apoptosis induction, which suggests that it may be a potential pharmacological agent in cancer therapy (8). Previous studies have demonstrated that GNA has lower toxicity and a wider spectrum of potent antitumor activity than GA (9,10). Additionally, GNA is able to inhibit cell proliferation in human hepatoma HepG2 cells via inducing cell apoptosis, and may be a possible pharmacological treatment strategy in HepG2 cells (6). GNA is able to induce G1 cell arrest in lung cancer cells via glycogen synthase kinase 3β-dependent cyclin D1 degradation and may have therapeutic potential in the treatment of lung cancer (11). GNA has also been demonstrated to serve a role in the apoptosis of U251 glioblastoma cells through inactivation of the protein kinase B (Akt) pathway (12). It has recently been demonstrated that GNA is associated with the induction of apoptosis in the B16 melanoma cell line (13). Despite these findings the regulatory mechanism by which GNA exerts its antitumor effects on choroidal melanoma progression has not yet been fully elucidated.

The present study aimed to explore the effects of GNA on the malignant behaviors of choroidal melanoma cells including cell growth, cell cycle, cell migration and invasion, and its regulatory mechanism. The findings of the present

study may serve as a theoretical basis for the development of an effective therapy for the treatment of choroidal melanoma.

Materials and methods

Cell culture. The human choroidal melanoma cell line OCM-1 was purchased from the American Type Cell Culture Collection (Manassas, VA, USA) and cultured at 37˚C for 24 h in RPMI-1640 medium (HyClone; GE Healthcare Life Sciences, Logan, UT, USA) supplemented with 100 μg/ml streptomycin, 100 U/ml penicillin, and 10% fetal bovine serum (FBS; Sigma-Aldrich; Merck Millipore, Darmstadt, Germany) at 37˚C in a humidified atmosphere containing 5% CO_2.

Cell viability assay. Cell viability was assessed via MTT assay performed as previously described with some modifications (14). Briefly, $1x10^4$ OCM-1 cells were seeded in triplicate into 96-well plates. Cells were incubated at 37˚C for 24 h in RPMI-1640 medium supplemented with different concentrations of GNA (0, 0.75, 1.5, 3, 4.5, and 6 μM; Sigma-Aldrich; Merck Millipore). A total of 50 μl MTT solution (Roche Applied Science, Penzberg, Germany) was added 24, 48 or 72 h post-treatment and cells were incubated at 37˚C for a further 4 h. A total of 150 μl dimethylsulfoxide was subsequently added to solubilize the formazan crystals. The optical density (OD) of each well was determined using a microplate reader (Bio-Rad Laboratories, Inc., Hercules, CA, USA). The cell viability ratio was calculated according to following formula: Cell viability rate (%) = OD of the experimental samples / OD of the control x100.

Colony formation assay. OCM-1 cells ($2x10^3$) were trypsinized and seeded in triplicate into six-well plates. Cells were cultured at 37˚C for 72 h in RPMI-1640 medium containing GNA of different concentrations (0, 0.75, 1.5, 3, 4.5, and 6 μM), which was replenished every two days. The resulting colonies were stained with 0.05% crystal violet and the number of colonies was counted using a microscope (Olympus Corporation, Tokyo, Japan).

Wound healing assay. A wound-healing assay was used to detect cell migration. Briefly, cells were treated with different concentrations of GNA (0, 0.75, 1.5, 3 μM) and seeded in triplicate in six-well plates at 37˚C for 24 h. When cells reached 90% confluence, a scrape wound was scratched on the cell layer using a sterile pipette tip. Cell migration ability was assessed by calculating the percentage of wound closure. The speed of wound closure was defined as the distance between wound edges from 0 to 72 h. Each experiment was conducted in triplicate.

Transwell invasion assay. The Transwell was coated with 0.1% gelatin (Sigma-Aldrich; Merck Millipore) for 30 min at 37˚C. Following three rounds of washing with PBS (pH 7.4), 100 μl OCM-1 cells ($4x10^4$ cells/well) was seeded into the top chambers of the Transwell, whereas the bottom chambers were filled with RPMI-1640 medium with 20% FBS. The top and bottom chambers contained the same series of concentrations of GNA (0, 0.75, 1.5, 3 μM). OCM-1 cells were incubated for 24 h at 37˚C and cells on the bottom side of the membrane, which were considered to be invading cells, were subsequently fixed with 4% paraformaldehyde at 37˚C for 20 min. Cells were washed with PBS three times and stained with 0.05% crystal violet for 10 min. Fields were selected at random, observed using an inverted light microscope (Olympus Corporation) and quantified by manual counting.

Cell cycle assay. OCM-1 cells ($1x10^5$) were seeded in six-well plates and treated with different concentrations of GNA (0, 0.75, 1.5, and 3 μM). Briefly, cells were harvested at 24 and 48 h post-treatment with GNA. Thereafter, the cells were washed with PBS, fixed with 70% ethanol at -20˚C for 24 h and centrifuged at 300 x *g* for 5 min. Then the cells were washed with PBS/1% bovine serum albumin (Sigma-Aldrich; Merck Millipore) and stained with 30 μg/ml propidium iodide containing 0.25 mg/ml RNase A for 30 min in the dark. The cell cycle assay was performed using the Propidium Iodide Nucleic Acid Stain kit (P3566; Invitrogen; Thermo Fisher Scientific, Inc., Waltham, MA, USA) in accordance with the manufacturer's protocol. Cell cycle distribution was analyzed using the FACSCalibur using Cell FIT software (Easy curve Fit 2.0) (both from BD Biosciences, San Jose, CA, USA).

RNA extraction and reverse transcription-quantitative polymerase chain reaction (RT-qPCR). OCM-1 cells ($1x10^5$) were grown in six-well plates, which were incubated with GNA (0, 0.75, 1.5, 3 μM) with or without LY294002 (15 mM; Sigma-Aldrich; Merck Millipore) for 24 h. LY294002, a specific inhibitor of the phosphoinositide 3-kinase (PI3K)/Akt signaling pathway, is able to significantly repress Akt phosphorylation (15). Total RNA was isolated from cells using TRIzol reagent (Invitrogen; Thermo Fisher Scientific, Inc.) and treated with DNase I. Purified RNA at density of 0.5 μg/μl with nuclease-free water was used for cDNA synthesis with the PrimeScript First Strand cDNA Synthesis kit (Invitrogen; Thermo Fisher Scientific, Inc.) according to the manufacturers protocol. Relative mRNA expression levels of cell cycle-associated proteins [cyclin D1, cyclin E, cyclin-dependent kinase (CDK) 2 and P21] and epithelial-mesenchymal transition (EMT)-associated molecules [epithelial (E)-cadherin, α-smooth muscle actin (SMA) and vimentin] were then determined via RT-qPCR assays using a SYBR-Green qPCR master mix kit (Toyobo Co., Ltd., Osaka, Japan) according to the manufacturer's protocol. The total reaction system of 20 μl volume was as follows: 1 μl cDNA, 10 μl SYBR Premix Ex Taq, 1 μl each of the primers (10 μM), and 7 μl ddH_2O. The primer sequences used for RT-qPCR amplification are presented in Table I. The amplification conditions were as follows: Denaturation at 95˚C for 30 sec, followed by 40 cycles of 95˚C for 5 sec, annealing at 60˚C for 30 sec, in which fluorescence signal was collected, and extension at 72˚C for 30 sec. The expression of GAPDH mRNA was used as internal control. Relative expression values from three independent experiments were analyzed by an ABI PRISM 7300 and calculated using the $2^{-\Delta\Delta Cq}$ method (16).

Western blot analysis. Cells treated with different concentrations of GNA (0, 0.75, 1.5, 3 μM) with or without LY294002

(15 μM) were lysed in ice-cold radioimmunoprecipitation assay buffer (Sigma-Aldrich; Merck Millipore) and the lysate was collected by centrifugation at 4,000 x *g* at 4˚C for 5 min. Protein concentration was determined using the bicinchoninic acid method. A total of 30 μg lysate was separated by 10% SDS-PAGE and transferred to polyvinylidene difluoride membranes (GE Healthcare Life Sciences). Membranes were subsequently blocked with 5% skimmed milk for 1 h at room temperature and probed with primary antibodies for PI3K (ab86714; 1:100), Akt (ab8805; 1:100), cyclin D1 (ab134175; 1:100), cyclin E (ab3927; 1:100), CDK2 (ab321147; 1:100) and P21 (ab109520; 1:100; all Sigma-Aldrich; Merck Millipore) at 4˚C overnight. Membranes were washed with Tris-buffered saline containing 0.1% Tween-20 and subsequently incubated at room temperature with anti-horseradish peroxidase-conjugated secondary antibodies against EPR3312 (ab197034; 1:1,000; Sigma-Aldrich; Merck Millipore) for 1 h. Protein blots were washed and visualized using an enhanced chemiluminescence detection (ECL) kit (Merck Millipore).

Statistical analysis. All values are expressed as the mean ± standard deviation calculated from three independent experiments. Student's *t*-test or one-way analysis of variance was performed using SPSS v17.0 software (SPSS, Inc., Chicago, IL, USA). P<0.05 was considered to indicate a statistically significant difference.

Table I. Primer sequences for reverse transcription-quantitative polymerase chain reaction.

Gene	Primer sequence (5'-3')
Cyclin D	F: GCCTCTAAGATGAAGGAGACCAT
	R: CATTTTGGAGAGGAAGTGTTCAAT
Cyclin E	F: GGATGTTGACTGCCTTGA
	R: CACCACTGATACCCTGAAA
CDK2	F: GCGAATTCCCCAGCCCTAATCTCA
	R: GCCTCGAGAACCCTCTTCAGCAATA
P21	F: ATGTCCAATCCTGGTGATGT
	R: TGCAGCAGGGCAGAGGAAGT
α-SMA	F: CCAGAGCAAGAGAGGGATCCT
	R: TGTCGTCCCAGTTGGTGATG
E-cadherin	F: CCAGTATCGTCCCCGTCCT
	R: CGGCTGCCTTCAGGTTTT
Vimentin	F: CGACAAGGTGCGCTTCCT
	R: CCTGGCCCTTGAGCTGC
GAPDH	F: TTCACCACCATGGAGAAGGC
	R: GGCATGGACTGTGGTCATGAG

CDK, cyclin dependent kinase; SMA, smooth muscle actin; E-cadherin, epithelial cadherin; F, forward; R, reverse.

Results

GNA inhibits the viability of OCM-1 cells in a dose-dependent manner. The results of the MTT assay demonstrated that the viability of OCM-1 cells was significantly inhibited with the increase in time and dosage of GNA treatment (P<0.01; Fig. 1A). Additionally, treatment with GNA resulted in a significant dose-dependent decrease in the colony formation ability of OCM-1 cells (P<0.01; Fig. 1B).

GNA induces G0/G1 arrest in a dose-dependent manner. Flow cytometry was used to investigate the effects of GNA on cell cycle (Fig. 2A). The results demonstrate that GNA gradually increased the proportion of OCM-1 cells in the G0/G1 phase in a dose-dependent manner. GNA concentration increased in a dose-dependent manner up to 1.5 μM (P<0.05) and increased further to 3.0 μM (P<0.01; Fig. 2B). Additionally, following GNA treatment, the cell cycle-associated molecules were found to have markedly decreased protein expressions (Fig. 2C) and the mRNA levels of these molecules significantly decreased in a dose-dependent manner compared with the control (Fig. 2D; P<0.01).

GNA may inhibit cell growth via inhibition of the PI3K/AKT pathway. To further explore the underlying mechanism for GNA-induced cell growth inhibition, LY294002, a specific inhibitor of the PI3K/Akt signaling pathway was used to treat cells. The results demonstrated that treatment with GNA or LY294002 resulted in a marked decrease in the protein expression of p-AKT/AKT (Fig. 3A). Furthermore, the combination of GNA and LY294002 treatment resulted in a marked decrease in p-AKT/AKT expression compared with the cells treated with GNA or LY294002 alone. Additionally, similar results were obtained regarding the expression of cell cycle-associated molecules cyclin D1, cyclin E, CDK2 and P21 (P<0.01; Fig. 3B), and cell viability (P<0.01; Fig. 3C).

GNA reduces the migration and invasion of OCM-1 cells. A wound healing assay was used to investigate cell migration following treatment with different concentrations of GNA, and the results demonstrated that treatment with GNA significantly reduced the migration ability of OCM-1 cells at all concentrations (P<0.05; Fig. 4A). Furthermore, the invasive ability of cells was assessed using Transwell assay, and the results revealed that the number of invasive cells was significantly reduced with GNA treatment (P<0.05; Fig. 4B). In order to further verify the association between GNA and the PI3K/AKT pathway, the expression of PI3K/AKT pathway-related protein was detected using western blot analysis. Cells were divided into four groups: Control, GNA (3 μM), LY294002 (15 μM) and GNA (3 μM) + LY294002 (15 μM). The protein and mRNA expressions of the EMT-associated proteins E-cadherin, α-SMA and vimentin were examined via RT-qPCR and western blotting, respectively. A significant dose-dependent increase in the mRNA levels of E-cadherin was observed with GNA treatment compared with the control group (P<0.01; Fig. 5A), whereas the levels of α-SMA and vimentin mRNA significantly decreased with GNA treatment in a dose-dependent manner (P<0.01; Fig. 5B and C). Similarly, western blot analysis demonstrated that levels of E-cadherin protein were markedly increased with increasing dosages of GNA, whereas protein levels of α-SMA and vimentin levels were markedly downregulated in a dose-dependent manner (Fig. 5D).

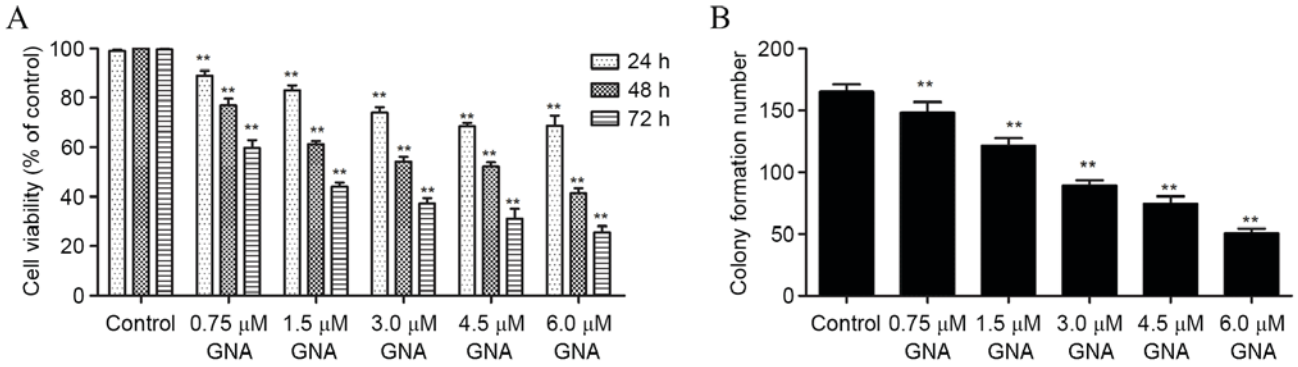

Figure 1. Effects of GNA on (A) cell viability and (B) colony formation ability. Data are presented as the mean ± standard deviation. **P<0.01 vs. control group. GNA, gambogenic acid.

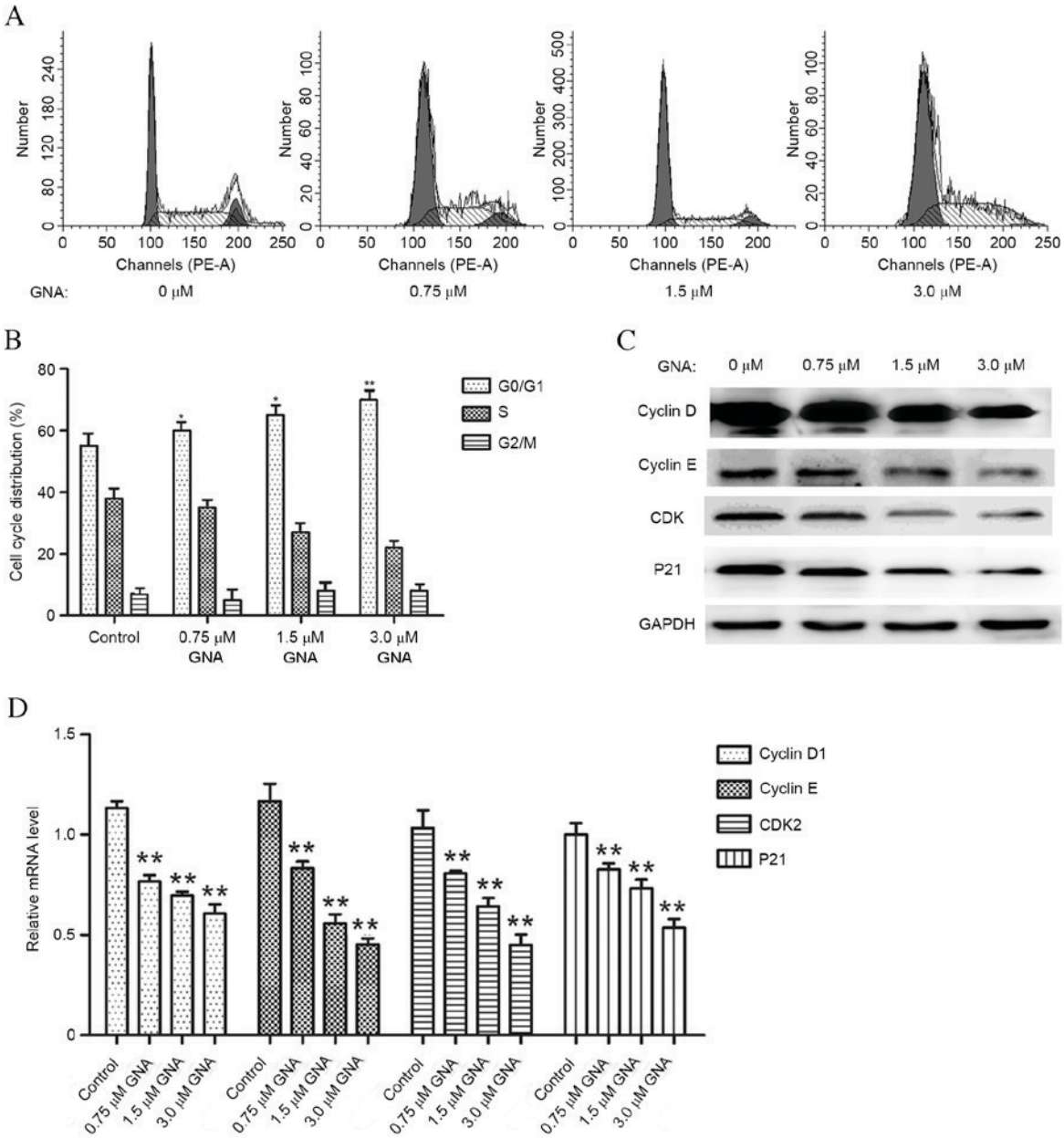

Figure 2. Effects of GNA on cell cycle. (A) Flow cytometry displayed the effects of GNA on cell cycle. (B) Cell cycle distribution. (C) Western blot analysis of cyclin D1, cyclin E, CDK2 and P21 proteins expressions. (D) Reverse transcription-quantitative polymerase chain reaction results for cyclin D1, cyclin E, CDK2 and P21 mRNA expressions. Data are presented as the mean ± standard deviation. *P<0.05; **P<0.01 vs. control group. GNA, gambogenic acid; CDK, cyclin dependent kinase.

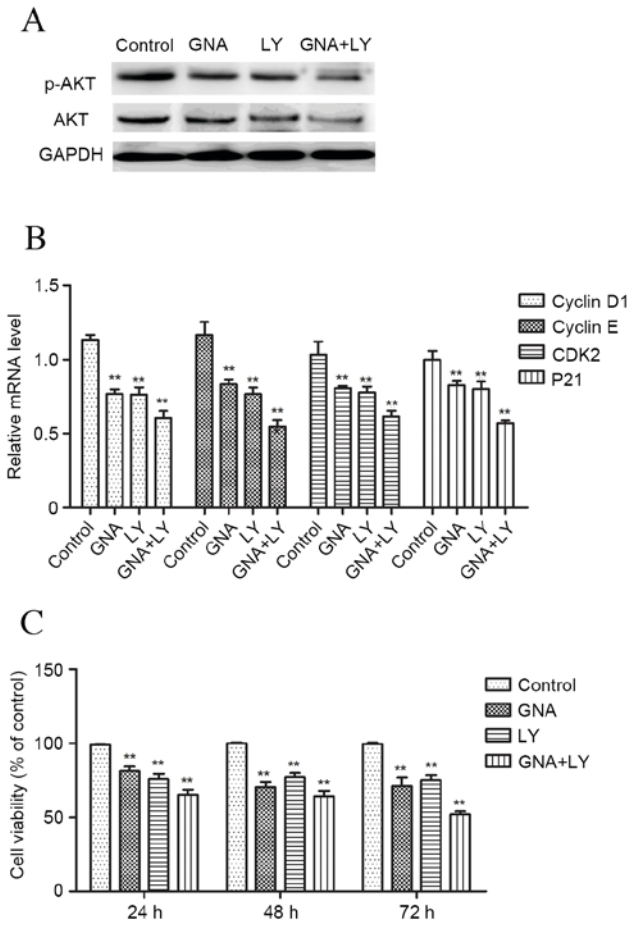

Figure 3. Effects of GNA and LY294002, a specific inhibitor of the PI3K/Akt signaling pathway, on cell growth. (A) The protein expression of p-AKT/AKT. (B) The expression of cell cycle-associated molecules (cyclin D1, cyclin E, CDK2 and P21) (C) MTT assay of cell viability. Data are presented as the mean ± standard deviation. **P<0.01 vs. control group. GNA, gambogenic acid; LY, LY294002; p, phosphorylated; PI3K, phosphoinositide 3-kinase; AKT, protein kinase B; CDK, cyclin dependent kinase.

Discussion

Choroidal melanoma is a serious metastatic malignant melanoma with poor prognosis (1). In recent years, increasing numbers of studies have been conducted to identify effective chemotherapy regimens with fewer side effects (2,4). In the present study, the effects of GNA on the malignant behaviors of choroidal melanoma cells and the possible underlying mechanisms were investigated. It was demonstrated that GNA was able to inhibit cell viability and induce cell cycle arrest at the G0/G1 phase in a dose-dependent manner via repressing the expression of cyclin D1, cyclin E, CDK2 and P21. Furthermore, GNA treatment suppressed cell migration and invasion in a dose-dependent manner. The results of the present study suggest that combined treatment with LY294002, which is a specific inhibitor of the PI3K/AKT pathway, and GNA exerts an additive effect on the growth of OCM-1 cells, which implies that the PI3K/AKT pathway may be an essential mechanism associated with GNA-induced growth inhibition.

GNA has previously been demonstrated to inhibit the proliferation of A549 cells via inducing cell cycle arrest (10). GNA is also able to inhibit cell proliferation, induce cell cycle arrest at G1 phase and suppress colony-forming activity of lung cancer cells (11). Consistent with these previous findings, the present study also demonstrated that GNA was able to inhibit OCM-1 cell growth and induce cell cycle arrest at the G0/G1 phase via repressing the expression of cyclin D1, cyclin E, CDK2 and P21. To further explore the possible mechanisms associated with GNA-induced growth inhibition and cell cycle arrest, the PI3K/AKT pathway specific inhibitor LY294002 was employed. The PI3K/AKT signaling pathway is crucial to the control of cell growth and survival (17). It has previously been demonstrated that the PI3K pathway is constitutively active in melanoma via increased expression of AKT and active AKT in the PI3K/ATK signaling pathway is able to increase cell proliferation and survival (18,19). Additionally, the PI3K/AKT pathway is also associated with cell cycle progression (20). AKT is able to induce pancreatic β-cell proliferation via regulating cell cycle components, such as cyclin D1, p21 and CDK4 (21). Furthermore, the PI3K/AKT pathway has previously been reported to serve an important role in melanoma initiation and therapeutic resistance (22). The results of the present study demonstrated that treatment with either GNA or LY294002 resulted in a marked decrease in p-AKT/AKT expression, whereas the combination of GNA and LY294002 was able to effectively inhibit the expression of p-AKT/AKT. Similar results were observed in the MTT assay, with the combined treatment resulting in a greater inhibition of the cell viability. It may therefore be suggested that treatment with GNA may inhibit cell growth and induce G0/G1 arrest in choroidal melanoma via involvement of the PI3K/AKT pathway, and that co-treatment with GNA and LY294002 may be an efficient therapeutic approach for the treatment of choroidal melanoma.

The metastatic activity of cancer cells is an important aspect of cancer progression. In the present study, it was demonstrated that the administration of GNA at different concentrations was able to reduce the migration and invasive ability of OCM-1 cells, which indicates that GNA may have an inhibitory role in tumor metastasis. Furthermore, the expressions of EMT-associated proteins (E-cadherin, α-SMA and vimentin) were examined. Studies revealed that EMT is a major contributor to the biological process of metastasis in a variety of cancers (23,24), including malignant melanoma (25). The upregulation of the EMT regulatory factor snail family transcriptional repressor 2, which is a transcriptional repressor of E-cadherin, functions as a precursor to the metastasis and invasion of melanoma (26), suggesting that decreased expression of E-cadherin may promote cell metastasis and invasion in malignant melanoma. Canel *et al* (27) demonstrated that the loss of E-cadherin function was correlated with tumor invasion and metastasis. Furthermore, it has previously been demonstrated that vimentin is overexpressed in malignant melanoma and its overexpression is correlated with accelerated tumor invasion and poor prognosis, suggesting that it may be a potential target for cancer therapy (28). Li *et al* (29) also demonstrated that vimentin may function as an indicator for melanoma hematogenous metastasis and poor prognosis. In the present study, the expression of E-cadherin markedly

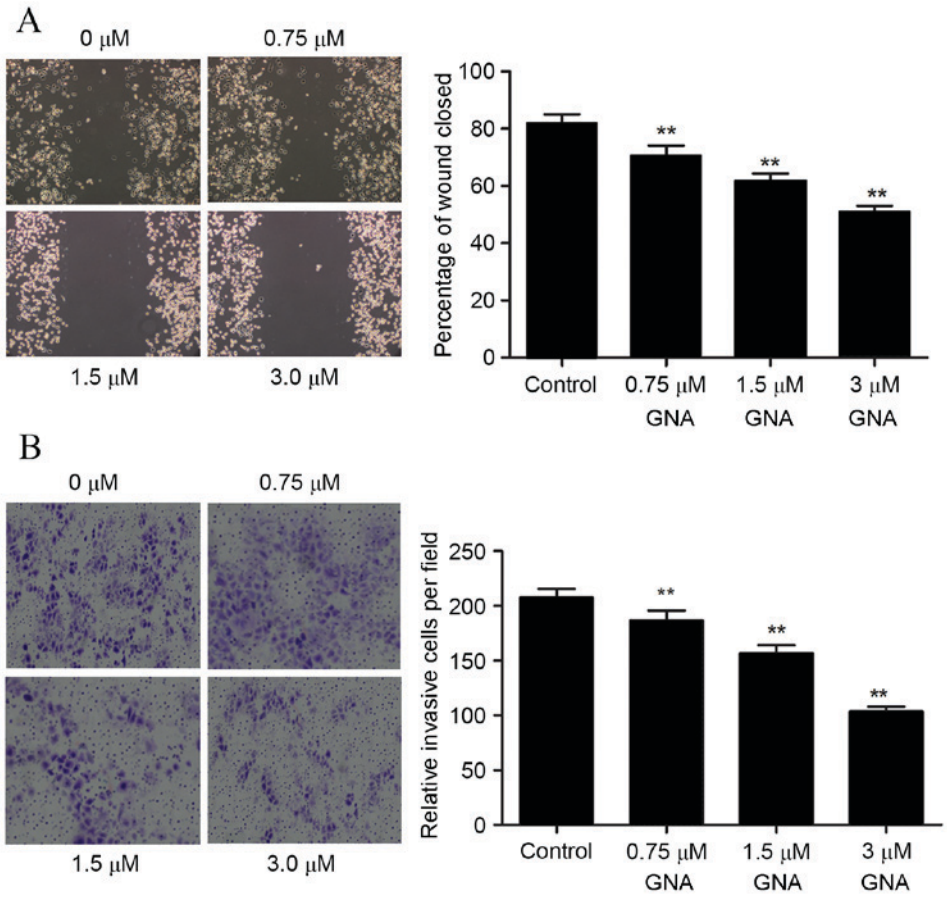

Figure 4. Effects of GNA on cell migration and invasion. (A) Wound healing assay of cell migration following treatment with different concentrations of GNA; (B) Transwell assay of invasive ability. Data are presented as the mean ± standard deviation **P<0.01 vs. control group. GNA, gambogenic acid.

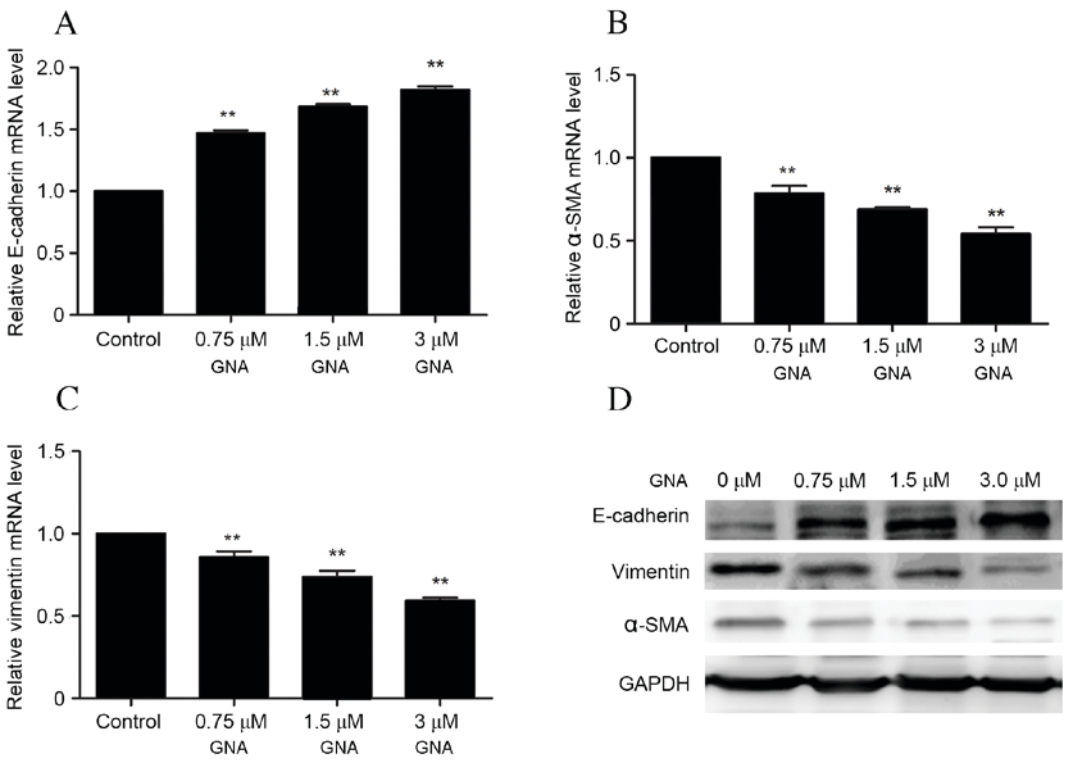

Figure 5. Effects of GNA on the mRNA expression of (A) E-cadherin, (B) α-SMA and (C) vimentin by reverse transcription-quantitative polymerase chain reaction analysis, and their (D) protein expression by western blot analysis. Data are presented as the mean ± standard deviation. **P<0.01 vs. control group. GNA, gambogenic acid; SMA, smooth muscle actin; E-cadherin, epithelial cadherin.

increased with the increase of the dose of GNA, whereas the expression levels of α-SMA and vimentin decreased in a dose-dependent manner. These results are in accordance with previous studies and suggest that GNA exerts an inhibitory effect on the metastasis of choroidal melanoma.

In conclusion, the findings of the present study indicate that GNA may inhibit cell growth and induce G0/G1 arrest. Furthermore, GNA may inhibit cell metastasis via regulating EMT-associated molecules. The PI3K/Akt signaling pathway may be a key mechanism involved in the development and progression of choroidal melanoma. GNA may serve as a potential therapeutic reagent for the treatment of this disease.

References

1. Shukla S, Acharya S and Dulani M: Choroid melanoma-A rare case report. J Clin Diagn Res 9: ED09-ED10, 2015.
2. Siegel R, Ma J, Zou Z and Jemal A: Cancer statistics, 2014. CA Cancer J Clin 64: 9-29, 2014.
3. Damato B, Eleuteri A, Taktak AF and Coupland SE: Estimating prognosis for survival after treatment of choroidal melanoma. Prog Retin Eye Res 30: 285-295, 2011.
4. Aubin JM, Rekman J, Vandenbroucke-Menu F, Lapointe R, Fairfull-Smith RJ, Mimeault R, Balaa FK and Martel G: Systematic review and meta-analysis of liver resection for metastatic melanoma. Br J Surg 100: 1138-1147, 2013.
5. Asadi S, Vaez-Zadeh M, Masoudi SF, Rahmani F, Knaup C and Meigooni AS: Gold nanoparticle-based brachytherapy enhancement in choroidal melanoma using a full Monte Carlo model of the human eye. J Appl Clin Med Phys 16: 5568, 2015.
6. Yan F, Wang M, Li J, Cheng H, Su J, Wang X, Wu H, Xia L, Li X, Chang HC and Li Q: Gambogenic acid induced mitochondrial-dependent apoptosis and referred to phospho-Erk1/2 and phospho-p38 MAPK in human hepatoma HepG2 cells. Environ Toxicol Pharmacol 33: 181-190, 2012.
7. Lu GB, Yang XX and Huang QS: Isolation and structure of neo-gambogic acid from Gamboge (*Garcinia hanburryi*). Yao Xue Xue Bao 19: 636-639, 1984 (In Chinese).
8. Wang X and Chen W: Gambogic acid is a novel anti-cancer agent that inhibits cell proliferation, angiogenesis and metastasis. Anticancer Agents Med Chem 12: 994-1000, 2012.
9. Qu BX: The experimental studies on antineoplastic action of gambogic II. Chinese J Clin Oncol 1: 021, 1991.
10. Li Q, Cheng H, Zhu G, Yang L, Zhou A, Wang X, Fang N, Xia L, Su J, Wang M, *et al*: Gambogenic acid inhibits proliferation of A549 cells through apoptosis-inducing and cell cycle arresting. Biol Pharm Bull 33: 415-420, 2010.
11. Yu XJ, Han QB, Wen ZS, Ma L, Gao J and Zhou GB: Gambogenic acid induces G1 arrest via GSK3β-dependent cyclin D1 degradation and triggers autophagy in lung cancer cells. Cancer Lett 322: 185-194, 2012.
12. Chen HB, Zhou LZ, Mei L, Shi XJ, Wang XS, Li QL and Huang L: Gambogenic acid-induced time- and dose-dependent growth inhibition and apoptosis involving Akt pathway inactivation in U251 glioblastoma cells. J Nat Med 66: 62-69, 2012.
13. Zhang X, Wang M, Cheng H, Su JJ and Li QL: Effect of gambogenic acid on apoptosis of melanoma cell line B16. J Anhui Traditional Chinese Med College 1: 020, 2013.
14. Nogami H, Hiraoka Y and Aiso S: Estradiol and corticosterone stimulate the proliferation of a GH cell line, MtT/S: Proliferation of growth hormone cells. Growth Horm IGF Res 29: 33-38, 2016.
15. Luo J, Manning BD and Cantley LC: Targeting the PI3K-Akt pathway in human cancer: Rationale and promise. Cancer Cell 4: 257-262, 2003.
16. Livak KJ and Schmittgen TD: Analysis of relative gene expression data using real-time quantitative PCR and the 2(-Delta Delta C(T)) Method. Methods 25: 402-408, 2001.
17. Hennessy BT, Smith DL, Ram PT, Lu Y and Mills GB: Exploiting the PI3K/AKT pathway for cancer drug discovery. Nat Rev Drug Discov 4: 988-1004, 2005.
18. Lejeune FJ, Rimoldi D and Speiser D: New approaches in metastatic melanoma: Biological and molecular targeted therapies. Expert Rev Anticancer Ther 7: 701-713, 2007.
19. Robertson GP: Functional and therapeutic significance of Akt deregulation in malignant melanoma. Cancer Metastasis Rev 24: 273-285, 2005.
20. Chang F, Lee JT, Navolanic PM, Steelman LS, Shelton JG, Blalock WL, Franklin RA and McCubrey JA: Involvement of PI3K/Akt pathway in cell cycle progression, apoptosis, and neoplastic transformation: A target for cancer chemotherapy. Leukemia 17: 590-603, 2003.
21. Fatrai S, Elghazi L, Balcazar N, Cras-Méneur C, Krits I, Kiyokawa H and Bernal-Mizrachi E: Akt induces beta-cell proliferation by regulating cyclin D1, cyclin D2, and p21 levels and cyclin-dependent kinase-4 activity. Diabetes 55: 318-325, 2006.
22. Davies MA: The role of the PI3K-AKT pathway in melanoma. Cancer J 18: 142-147, 2012.
23. Yang J and Weinberg RA: Epithelial-mesenchymal transition: At the crossroads of development and tumor metastasis. Dev Cell 14: 818-829, 2008.
24. Thompson EW, Newgreen DF and Tarin D: Carcinoma invasion and metastasis: A role for epithelial-mesenchymal transition? Cancer Res 65: 5991-5995, 2005.
25. Caramel J, Papadogeorgakis E, Hill L, Browne GJ, Richard G, Wierinckx A, Saldanha G, Osborne J, Hutchinson P, Tse G, *et al*: A switch in the expression of embryonic EMT-inducers drives the development of malignant melanoma. Cancer Cell 24: 466-480, 2013.
26. Fenouille N, Tichet M, Dufies M, Pottier A, Mogha A, Soo JK, Rocchi S, Mallavialle A, Galibert MD, Khammari A, *et al*: The epithelial-mesenchymal transition (EMT) regulatory factor SLUG (SNAI2) is a downstream target of SPARC and AKT in promoting melanoma cell invasion. PLoS One 7: e40378, 2012.
27. Canel M, Serrels A, Frame MC and Brunton VG: E-cadherin-integrin crosstalk in cancer invasion and metastasis. Journal of cell science 126: 393-401, 2013.
28. Satelli A and Li S: Vimentin in cancer and its potential as a molecular target for cancer therapy. Cellular and Molecular Life Science 68: 3033-3046, 2011.
29. Li M, Zhang B, Sun B, Wang X, Ban X, Sun T, Liu Z and Zhao X: A novel function for vimentin: The potential biomarker for predicting melanoma hematogenous metastasis. J Exp Clin Cancer Res 29: 109, 2010.